

### **ARTICLE TYPE**

Cite this: DOI: 00.0000/xxxxxxxxxx

# Stability Study of Molecularly-Doped Semiconducting Polymers

Meghna Jha $^a$ , Joaquin Mogollon Santiana $^a$ , Aliyah A. Jacob $^b$ , Kathleen Light $^a$ , Megan L. Hong $^b$ , Michael R. Lau $^b$ , Leah R. Filardi $^a$ , Haoqian Miao $^c$ , Sadi M. Gurses $^a$ , Coleman X. Kronawitter $^a$ , Mark Mascal $^c$ , Adam J. Moule\* $^a$ 

Received Date Accepted Date

DOI: 00.0000/xxxxxxxxxx

Abstract: Molecular doping of semiconducting polymers has emerged as a prominent research topic in the field of organic electronics with new dopant molecules introduced regularly. FeCl<sub>3</sub> has gained attention as a p-type dopant due to its low-cost, availability, ability to dope high ionization energy copolymers, and its use as a dopant that can be used with anion exchange. Here, we use a combination of UV-Vis-NIR spectroscopy, four-probe sheet resistance measurements, and X-ray absorption nearedge structure (XANES) spectroscopy to perform lifetime measurements to assess the stability of the doped polymers over time, which is crucial for evaluating the long-term performance and reliability of the doped films. We used gas chromatography-mass spectrometry (GCMS) to prove that FeCl<sub>3</sub> can cause radical side reactions that damage the conjugated polymer backbone, leading to degradation of the electronic properties. The rate of this degradation is orders of magnitude higher when the film is exposed to air. Anion exchange doping can reduce the [FeCl<sub>4</sub>] concentration, but does not necessarily improve the doping lifetime because anion exchange electrolytes can serve as co-reactants for the degradation reaction. By comparison, doping with (2,3,5,6-tetrafluoro-2,5-cyclohexadiene-1,4-diylidene)dimalononitrile (F4TCNQ) as the reactive dopant results in lower initial conductivity, but the lifetime of the doped polymer is almost tripled as compared to FeCl<sub>3</sub> doped polymer films. These findings highlight that the use of FeCl<sub>3</sub> as a molecular dopant requires a cost/benefit analysis between higher initial doping levels and lower film stability.

#### 1 Introduction

Semiconducting polymers (SPs) have received widespread attention due to their promising qualities like superior absorbance/emission compared to inorganic semiconductors, easy chemical tunability, low-temperature solution processing, light weight, flexibility, and low environmental toxicity. <sup>1–3</sup> Like inorganic semiconductors, the electronic properties of SPs can be controlled using a doping process. But unlike inorganic semiconductors, the dopants are added molecules instead of added atoms. Molecular doping involves a redox reaction between the polymer and the dopant. Typically, a p-type molecular dopant is a oxidizing agent that removes an electron from the conjugated core of the polymer resulting in a hole or a positive charge on the

FeCl<sub>3</sub> (Fig. 1a) has been reported as a low-cost and efficient p-type chemical dopant for SPs. Several groups have reported a very high conductivity  $\sim 900$  S/cm when using FeCl<sub>3</sub> to dope SPs. <sup>8,9</sup> Zeng et al. demonstrated an n-type-like oriented and conducting polymer using p $\rightarrow$ n polarity switching of films of doped DPP-5T (a donor/acceptor co-polymer) by varying the concentration of the FeCl<sub>3</sub>. <sup>9</sup> Liang et al. report the electron affinity of FeCl<sub>3</sub> to be 4.6 eV w.r.t. vacuum, which is not high enough to achieve ionization of high IP co-polymers as has often been reported. <sup>7</sup> Jacobs et al.

polymer backbone and a negatively charged counter ion.  $^{1,2}$  The electron affinity (EA) of the dopant must be higher than the ionization potential (IP) of the polymer by  $\sim 0.11$  eV for efficient electron transfer to occur.  $^{2,4}$  Increasing the EA of the dopant leads to more efficient polaron or bipolaron formation but can often lead to chemical instability of the dopant molecule itself.  $^5$  Anion exchange doping was recently introduced as a method to replace the redox active dopant counter ion with a stable ion, but no lifetime or diffusion tests have been published.  $^6$  The chemical stability of doped SPs remains a huge concern for the field  $^{7,8}$  and is the main subject of this article.

<sup>&</sup>lt;sup>a</sup> Department of Chemical Engineering, University of California Davis, One Shields Avenue, Davis, California 95616, USA. Phone: +1(530)754-5373; E-mail: amoule@ucdavis.edu

b Department of Material Science and Engineering, University of California Davis, One Shields Avenue, Davis, California 95616, USA

<sup>&</sup>lt;sup>c</sup> Department of Chemistry, University of California Davis, One Shields Avenue, Davis, California 95616, USA

report that [FeCl<sub>4</sub>] is the resulting counter ion from FeCl<sub>3</sub> doping, suggesting that the doping effectiveness is a result of a more complex electrochemical reaction. FeCl<sub>3</sub> has also been used in combination with other materials like concentrated electrolytes to achieve increased doping levels and high conductivity. FeR Yamashita et al. first proposed the anion exchange technique to achieve higher doping levels using a combination of a molecular dopant and a concentrated electrolyte. This mechanism is a two-step process that occurs in a single solution. The two steps that occur in anion exchange molecular doping are:

- 1. **Charge transfer:** The p-type molecular dopant (like FeCl<sub>3</sub> or F4TCNQ) oxidizes the polymer backbone through a reversible electron transfer process.
- 2. **Anion exchange:** The dopant counter ion exchanges with an electrolyte counter ion, typically due to a much higher concentration of the electrolyte anion in solution.

Anion exchange doping is thought to deliver a higher doping level than molecular doping because the anion exchange counter ion is unable to undergo back reaction. <sup>6,8,10</sup> In contrast, the counter ion for a molecular dopant is intrinsically in equilibrium and thus the population is never 100% ionized. <sup>4</sup> In addition, anion exchange enables the choice of chemically stable counter ions or counter ions with a different size/shape. Hence, anion exchange doped samples should have longer operational lifetime and give much greater morphological control of the resulting film. It is known that counter ions effectively intercalate into the lamellae of the polymer. <sup>8,11–13</sup> A larger counter ion should also reduce the diffusion and drift rates of the anion in the film. <sup>14–16</sup> On the other hand, a larger counter ion increases the film volume, reducing the volumetric charge density. <sup>17</sup>

In this article, we first study the stability of the dopant FeCl<sub>3</sub> in the semiconducting co-polymer PDPP-4T by cycling doping and de-doping. We also examine anion exchange in films that were doped with FeCl<sub>3</sub> with an excess LiTFSI. For all films doped using FeCl<sub>3</sub>, the conductivity steadily decreases in an inert environment and much more quickly with exposure to O<sub>2</sub> and H<sub>2</sub>O. Our findings indicate that a side product of doping with FeCl<sub>3</sub> are radicals that can damage the conjugated backbone of the polymer. <sup>18,19</sup> Anion exchange does not fully remove the [FeCl<sub>4</sub>] and so any use of FeCl<sub>3</sub> results in this damaging side reaction. We conclude by comparing P3HT films anion exchange doped using FeCl<sub>3</sub> and F4TCNQ. Although the FeCl<sub>3</sub> doped films have initially higher conductivity, the films doped with F4TCNQ have a much longer doping lifetime because the adverse side reaction is avoided.

#### 2 Materials and Methods

Materials: PDPP-4T was supplied from Osilla and P3HT was supplied from Sigma Aldrich. n-Butyl acetate, acetonitrile, FeCl<sub>3</sub> and LiTFSI were purchased from Sigma Aldrich. Borosilicate glass microscope slides (Fischer Scientific) cut to the required size were used as the substrates. All substrates were cleaned by ultrasonication in acetone, methanol, isopropyl aclochol and de-ionised water for 10 minutes each. They were then dried with compressed N<sub>2</sub> and UV-ozoned for 20 minutes.

- 2. Thin film preparation: All polymer thin films used in this paper were spin coated in a  $N_2$  glove box and were  $\sim 100$  nm thick. PDPP-4T films were coated at 1300 rpm for 90 s from a 5 mg/ml 4:1 chloroform:chlorobenzene solution. P3HT films were coated at 1000 rpm for 90s from a 25 mg/ml dichlorobenzene solution. All films were annealed at 125 °C for 1 hour on a hot plate after spin coating.
- 3. Doping solutions used: 5 mM FeCl<sub>3</sub> solutions prepared in anhydrous acetonitrile were used to dope PDPP-4T and P3HT. For anion exchange, a mixture of 5 mM FeCl<sub>3</sub> and 100 mM LiTFSI was used. All doping solutions were prepared inside a N<sub>2</sub> glove box.
- 4. Doping experiments: All doping experiments were carried out in vials inside the  $N_2$  glove box. Each vial was filled with enough doping solution ( $\sim$ 8 ml) to cover the entire substrate and was allowed to rest for 5 minutes and reach equilibrium doping levels. These doped films were then spun coated at 2000 rpm for 60 s to remove any excess dopant solution.
- 5. XANES experiments: X-ray absorption near-edge structure (XANES) spectroscopy of the Fe L-edge, F K-edge and C K-edge regions were conducted at beamline 7.3.1 of the Advanced Light Source (ALS), Lawrence Berkeley National Laboratory. The polymer films were deposited on a conductive ITO substrate. The samples were transferred from a glove box to the UHV XAS analysis chamber with an air-free vacuum suitcase. The energy resolution was set to 0.2 eV at all edges. Spectra of total electron yield (TEY) were collected and energy-corrected by referencing standards of Fe<sub>2</sub>O<sub>3</sub> <sup>20</sup> and HOPG <sup>21</sup> to known values for the Fe L<sub>2,3</sub> and C 1s edges, respectively. The TEY signal was normalized to the incident photon beam. Athena (XAS data processing) software was used for linear pre-edge and post-edge normalization of the Fe L<sub>2</sub> and L<sub>3</sub> edges.
- 6. Gas Chromatography-Mass Spectrometry: A Shimadzu-QP2010 SE GC-MS instrument was used in this experiment. The samples were subjected to a preparation process which involved dilution with ethyl acetate followed by a DI water extraction to remove inorganic salts. The resulting organic phases were then dried over sodium sulfate. Prior to injection, all samples were passed through syringe filters with a pore size of 0.45 micrometers (PTFE, Millipore Millex-FH).

#### 3 Results and Discussion

#### 3.1 PDPP-4T doped with FeCl<sub>3</sub>

First, sequentially solution the alternatdoped donor/acceptor (D/A)co-polymer poly[2,5-bis(2octyldodecyl)pyrrolo[3,4-c]pyrrole-1,4(2H,5H)-dione-3,6diyl)-alt-(2,2';5',2";5",2"'-quaterthiophen-5,5"'-diyl)] (PDPP-4T) with the p-type molecular dopant FeCl<sub>3</sub> (anhydrous), as depicted in Fig. 1a. PDPP-4T is a well studied alternating electron donor/acceptor semiconducting co-polymer, which has a small optical band gap and high charge carrier mobility. 22 Alternating co-polymers of this kind typically have high IE and present challenges in terms of molecular doping. 23 Fig. 1b shows the UV-Vis-NIR absorption spectra of a PDPP-4T film before (black spectrum) and after (red spectrum) sequentially doping with a 5 mM solution of FeCl<sub>3</sub> in acetonitrile (AN). The undoped film shows a strong vibronic absorption with maximum absorbance at ~1.6 eV. PDPP-4T is an H-aggregate characterized by stronger absorbance in the second vibronic peak compared to the first. 24,25 The broad absorbance between 2.25-3.25 eV comes from the homo-interactions between acceptors (A-A) and donors (D-D). 26 Sequential doping with 5 mM FeCl<sub>3</sub> results in almost complete bleaching of the neutral peaks at around 1.43 (0-0), 1.57 (0-1), and 1.64 (0-2) eV. Simultaneously new absorption peaks at 0.33 (P1), 0.88 (P2), and 1 (P3) eV have been assigned to polaron absorbance from PDPP-4T+.4,27 The change in spectra are consistent with polaron formation on the polymer and complete ionization of the dopant molecule. <sup>28,29</sup> In addition to the expected polymer polaron peaks, there are additional weak absorbance peaks at ~3.4 eV and ~4.0 eV that come from the FeCl<sub>3</sub> dopant, discussed in detail below. <sup>8,30</sup>

To investigate anion exchange, PDPP-4T was also doped with a mixture of 5 mM  $\rm FeCl_3+100$  mM LiTFSI. From now on, for simplicity, we refer to  $\rm FeCl_3$  doped SPs as "w/o anion exchange (AE)" and  $\rm FeCl_3+LiTFSI$  doped SP as "w/ AE". Fig. 1b also shows the UV-Vis-NIR spectra of PDPP-4T w/ AE (blue spectrum). Here, LiTFSI (lithium bis(trifluoromethane)sulfonimide, structure shown in Fig. 1a) was used as the anion exchange electrolyte. There are several advantages of using LiTFSI. For example, the TSFI $^-$  ion interacts weakly with cations and is stable under oxidizing conditions.  $^{6,8}$ 

To test the stability of doped PDPP-4T films w/o AE and w/ AE under oxidizing conditions, the film was allowed to de-dope in air while being covered to prevent exposure to light. The degradation of the doped films was monitored by periodically taking UV-Vis-NIR spectra and four-bar conductivity measurements. Fig. 1b shows the UV-Vis-NIR spectra of PDPP-4T w/o AE (solid red) and w/ AE (solid blue) directly after doping and after they were completely de-doped in air in the dark (dashed red and blue spectra). The neat film absorbance is unchanged over hundreds of hours in air in the dark (See Supporting Information Figure S1). For the doped films w/o AE and w/ AE, the neutral polymer absorbance peaks ~1.6 eV are significantly reduced in intensity compared to the original un-doped, neat film (dashed red, dashed blue vs. black spectra). We can be sure that the films are entirely de-doped because the polaron absorbance returns to the same baseline absorbance in the near IR as the neutral film.

Fig. 1c is a plot of the normalized optical density (O.D.) of the neutral PDPP-4T absorbance at  $\sim 1.6$  eV vs time. It shows the growth of the neutral peak for PDPP-4T w/o and w/ AE during de-doping time. The O.D. is normalized w.r.t. the neutral peak of undoped, neat PDPP-4T. The black stars at normalized O.D. = 1 represent that the neat polymer does not degrade during the process. By comparison, the neutral absorbance does not recover completely for either doped sample. We controlled the film thickness and can verify that no polymer was lost in the doping process. Thus we can conclude that the polymer absorbance is bleached over time for all FeCl<sub>3</sub> samples doped w/o and w/ AE.

In this comparison, using anion exchange to exchange TFSI<sup>-</sup> for [FeCl<sub>4</sub>]<sup>-</sup> does not result in an extended lifetime. In fact, using AE resulted in more bleaching of the neutral peak than without AE, which contradicts the hypothesis that exchanging [FeCl<sub>4</sub>]<sup>-</sup> for TFSI<sup>-</sup> will result in more stable doping.

The reduction in neutral absorbance in the doped film could come from one of three mechanisms: (1) the film could have lost thickness during sequential doping with the FeCl<sub>3</sub> solution, (2) the polymer was degraded during the doping step, or (3) the polymer was degraded while de-doping in air. We looked at each possibility one by one.

- 1. The thickness was measured before and after doping (see Supporting Information Section S1). We found that the layer thickness was the same within 5% error. We can safely conclude that the 25% reduction in the neutral peak absorbance is not due to a change in the film thickness.
- 2. An undoped PDPP-4T film does not bleach in air in the dark for at least 100 hours (see Supporting Information Figure S1). Degradation during sequential doping was measured by taking absorbance measurements of the sequentially doped PDPP-4T film with FeCl<sub>3</sub> after it was chemically de-doped using butyl-amine (See Supporting Information Section S2). This data shows negligible change in absorbance for the chemically de-doped film, which proves that sequential doping with FeCl<sub>3</sub> is not responsible for degradation of the PDPP-4T absorbance. The degradation only occurs over time in the presence of FeCl<sub>3</sub>.
- 3. The third possibility is that neutral sites on the polymer backbone are degraded (double bonds are broken) while the doped polymer film sits in air. The increased absorbance between 2.25-4.00 eV for the red spectrum in Fig. 1b also suggests the presence of some other chemical species in the de-doped films.

Based on these results, we hypothesize that the Fe dopant undergoes an unwanted side reaction while in contact with air that results in degradation of the polymer backbone. To test this hypothesis, a PDPP-4T film was doped with 5 mM FeCl<sub>3</sub>, allowed to de-dope in air (red spectrum in Fig. 1d), then doped again with 5 mM FeCl<sub>3</sub> and allowed to de-dope in air again (brown spectrum in Fig. 1d). The doping and de-doping cycles were repeated three times, with UV-Vis-NIR measurements after each cycle. The UV-Vis-NIR absorption spectra are shown in Fig. 1d. A reduction in the neutral peak at  $\sim$ 1.6 eV and an increase in absorbance around 2.25-4.0 eV was observed for each sequential cycle. The total film thickness of the doped film remains constant with each doping/de-doping cycle. Fig. 1e shows the reduction in O.D. of the neutral peak with each de-doping cycle. There is more than 80% reduction in the absorbance of PDPP-4T after three doping/de-doping cycles. This proves that each time the polymer de-dopes in air, some bonds on the polymer backbone are broken, reducing the neutral absorbance. The increased absorbance at 2.25-4.0 eV is likely due to remaining partially conjugated polymer chain segments and the FeCl<sub>3</sub> dopant molecules/radicals.

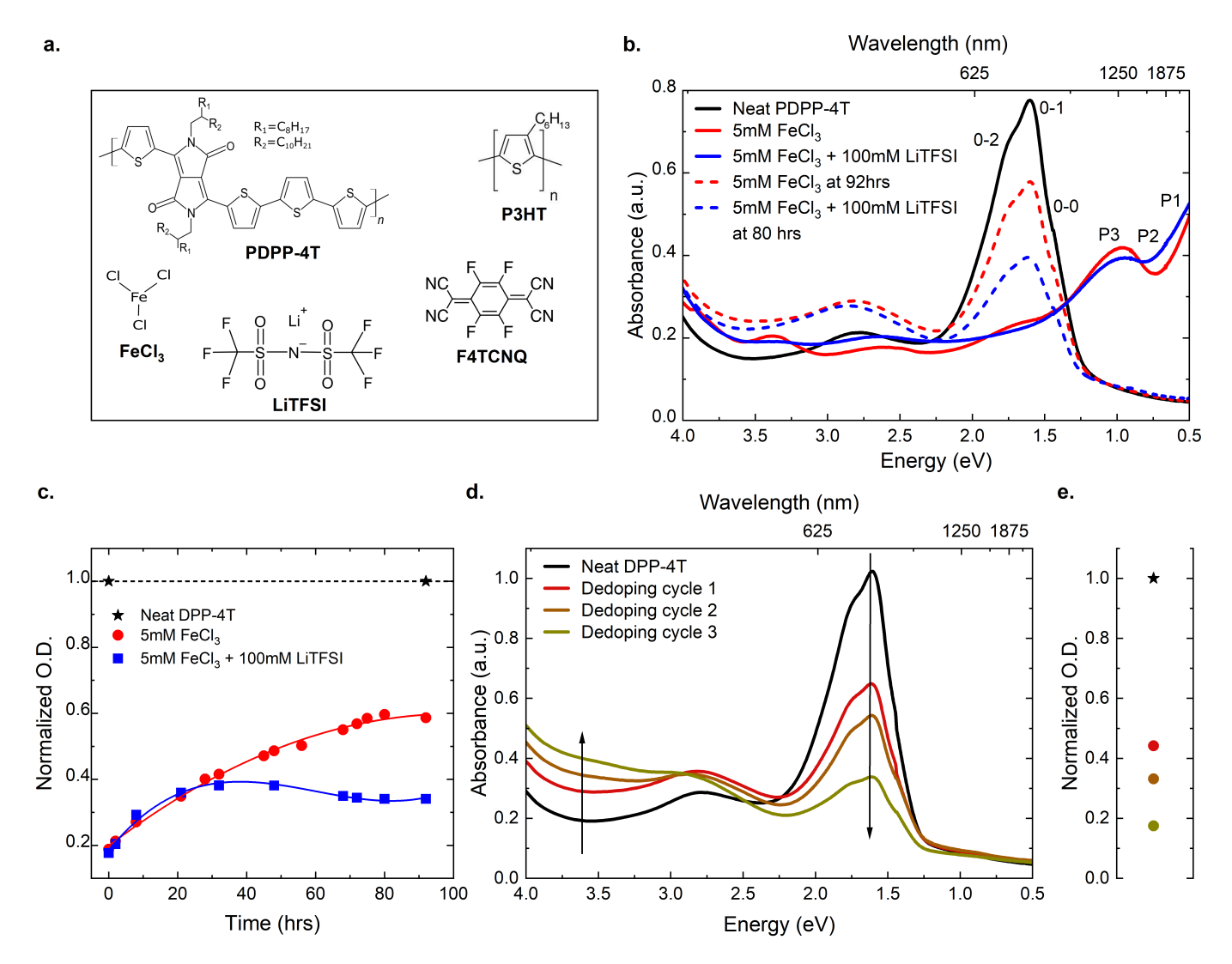


Fig. 1 a) Molecular structures of PDPP-4T, P3HT, FeCl<sub>3</sub>, LiTFSI, F4TCNQ. b) UV-Vis-NIR absorption spectra of PDPP-4T neat (black), doped with 5 mM FeCl<sub>3</sub> and either 0 (red) or 100 (blue) mM LiTFSI at t=0 (solid) and de-doped in air (dashed). c) Plot of normalized optical density (O.D.) of growth of the neutral peak of PDPP-4T versus de-doping time for a film in air. d) UV-Vis-NIR absorption spectra of PDPP-4T, neat (black) and de-doped in air after multiple cycles of solution doping (red, brown, yellow). e) Decrease in O.D. of the neutral peak in (d) over de-doping cycles.

In order to better understand the degradation of PDPP-4T films after doping, conductivity was repeatedly measured using fourpoint probe on the films while they de-doped in air and in a N2 glovebox. Fig. 2a is the loglog plot of conductivity vs time for PDPP-4T w/o AE (red) and w/ AE (blue). The decrease in conductivity over time can be described by two rates, which are seen as changes in the slope: r1 and r2. These are tabulated in Table 1. For detailed calculation of the rates, refer to Supporting Information Section S4. At early times, all samples undergo a burn-in or initial reduction in conductivity, r<sub>1</sub>, that is higher in samples exposed to air. After 10-15 hours, a second mechanism becomes dominant both in air and in the N2 glove box which is described by r<sub>2</sub>. A second systematic observation is that the conductivity reduces faster w/ AE than without. This means that the goal of AE, which is to substitute a more stable anion in place of the unstable [FeCl<sub>4</sub>]<sup>-</sup>, is not fully accomplished. Third, the initial conductivity (at t=0) of the film w/o AE (117.6 S/cm) is higher than the one w/ AE (29.4 S/cm), which is not consistent with previously published anion exchange results.  $^{6,10}$ 

Anion exchange has been tested sporadically with different dopants, exchange anions, solvents, and polymers. A more critical review of literature shows that Murrey et al. report an increase in conductivity for the polymer PDPP-2T with AE using n-butyl acetate (nBA) as a solvent but a decrease for P3HT at low concentrations of FeCl<sub>3</sub>. <sup>10</sup> Jacobs et. al. show a decrease in conductivity for PBTTT with AE using FeCl<sub>3</sub> as dopant and BMP TFSI (1-butyl-1-methylpyrrolidinium bis(trifluoromethylsulfonyl)imide) as anion exchange electrolyte in an acetonitrile (AN) solution at low concentrations. <sup>8</sup> Yamashita et. al. show a large increase in conductivity in the polymer PBTTT using F4TCNQ and TFSI<sup>-</sup> as a dopant and anion with nBA as the solvent. In preparing this publication, we found that FeCl<sub>3</sub> disproportionates more effectively in AN but not nBA because AN has a high dielectric constant of 40 while that of nBA is only 5.1. This means that any doping

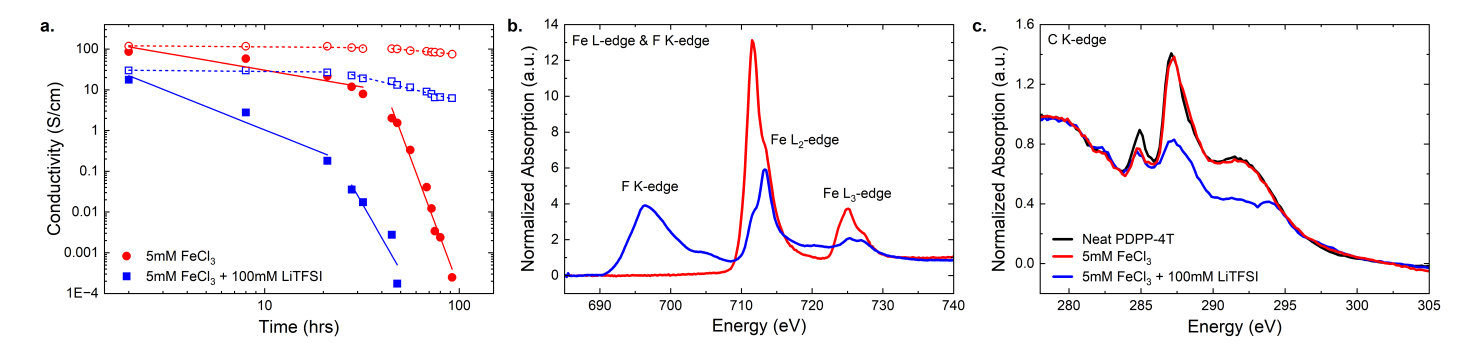


Fig. 2 PDPP-4T w/ and w/o AE a) Four probe conductivity measurements of PDPP-4T doped with 5 mM FeCl<sub>3</sub> and 0 (red) and 100 mM (blue) LiTFSI over de-doping time (solid symbols for air and hollow symbols for  $N_2$ ). b) XANES Fe-L edge and F K-edge for PDPP-4T doped with 5mM FeCl<sub>3</sub> and 0 (red) or 100 mM (blue) LiTFSI. c) XANES C K-edge for DPP-4T neat (black), doped with 5mM FeCl<sub>3</sub> and either 0 (w/o AE, red) or 100 mM (w/ AE, blue) LiTFSI.

process with FeCl<sub>3</sub> is more effective in AN than in nBA. Fig. 3a is the absorption spectra of FeCl<sub>3</sub> in AN and nBA. The shape of the spectra is completely different because FeCl3 remains mostly neutral in nBA but disproportiionates in AN. These doping solutions were then used to dope neat PDPP-4T. The UV-Vis-NIR spectra of neat PDPP-4T (black), doped with 5 mM FeCl<sub>3</sub> from AN (purple) and doped with 5 mM FeCl<sub>3</sub> from nBA (green) are shown in Fig. 3b. The FeCl<sub>3</sub> solution from AN completely bleaches the neutral peak of the polymer while the FeCl<sub>3</sub> solution from nBA does not. For both solutions, the reduction of the dopant species causes the doping of the polymer. However, since AN causes more disproportionation of FeCl<sub>3</sub> in solution, a higher concentration of the dopant species is available and therefore, a much higher doping level is achieved. With this added perspective, our data is consistent with past results. Sequential doping with FeCl3 in AN produces the high initial conductivity. AE with TFSI- results in a lower conductivity but a similar optical doping level as measured by UV-Vis-NIR spectroscopy.

To determine the reasons that AE results in lower initial conductivity and faster reduction of the conductivity with time, it is necessary to better understand the doping species present in the film. Doping with FeCl<sub>3</sub> results in [FeCl<sub>4</sub>] counter ions.<sup>8</sup> Presumably various other Fe ions with Cl are present in addition to [FeCl<sub>4</sub>]<sup>-</sup>. The UV-Vis-NIR spectra in Fig. 1b for both w/ AE and w/o AE samples show a peak at  $\sim$ 3.44 eV, which is an indication of [FeCl<sub>4</sub>] - (for detailed fits see Supporting Information Figure S3). To corroborate this, we performed X-ray absorption near-edge structure (XANES) spectroscopy to detect the Fe species present in the doped films. Fig. 2b is the Fe L-edge and F K-edge XANES spectra of PDPP-4T w/ (blue spectrum) and w/o (red spectrum) AE shortly after doping. PDPP-4T w/ AE (blue spectrum) shows the Fe L<sub>2</sub> and L<sub>3</sub>-edges at  $\sim$ 712 eV and  $\sim$ 725 eV respectively along with a F K-edge peak at around ~697 eV. The F K-edge is only seen in the w/ AE sample because the fluorine is introduced via the TFSI<sup>-</sup> ion. It is evident from this plot that PDPP-4T w/ AE contains both iron and fluorine signals which most likely come from [FeCl<sub>4</sub>] and TFSI ions respectively. This means that anion exchange is not 100% and [FeCl<sub>4</sub>] - persists in the anion exchanged film.

In order to get an insight into the change in the local structure

	Sample	$r_1\left[\frac{1}{hr}\right]$	$r_2 \left[\frac{1}{hr}\right]$
П	PDPP-4T w/o AE in N <sub>2</sub>	0.00025	0.0034
$\prod$	PDPP-4T w/ AE in N <sub>2</sub>	0.0013	0.04
$\llbracket$	PDPP-4T w/o AE in air	0.0095	0.15
П	PDPP-4T w/ AE in air	0.11	0.48

Table 1 Decay rates for degradation of PDPP-4T doped using  ${\sf FeCl}_3$  as the reactive dopant.

upon doping, we also look at the carbon K-edge XANES spectrum. Fig. 2c is the C K-edge of the PDPP-4T, neat (black), w/o AE (red) and w/ AE (blue) (t=3-4 hrs). The peak around 285 eV is assigned to C 1s which refers to the unoccupied states of the C=C  $\pi^*$  character, where the intensity of the peak signifies the density of unoccupied  $\pi^*$  states.  $^{21,32,33}$  The peaks between 287 eV and 290 eV are assigned to C=O  $\pi^*$ , C-H  $\sigma^*$  and C-C  $\sigma^*$  bands. All the peaks starting 292 eV are other  $\sigma^*$  bands like C-N, C-S.  $^{21,32,33}$ The relative reduction in intensity for the AE sample indicates one of the following: (1) Since the relative intensity of the unoccupied states decreases, there may be addition of electrons in the AE sample. (2) There is significantly lower carbon density at the surface of this sample, which means that either the TFSI<sup>-</sup> ions cover the surface of the AE film or the sample contains less carbon overall. Since LiTFSI only acts as an anion exchange electrolyte and does not play any role in the doping itself, it is more likely that the huge decrease in peak intensity for the AE sample points towards the possibility of the sample surface being covered by TFSI- ions.

Summarizing the lifetime results for PDPP-4T, there is a reaction that occurs in the presence of air with  $[FeCl_4]^-$  that results in breaking conjugated bonds in the polymer. We used AE to try to remove the  $[FeCl_4]^-$  and replace it with  $TFSI^-$ . The exchange reaction was incomplete resulting in a mix of  $[FeCl_4]^-$  and  $TFSI^-$  counterions. The AE sample has lower initial conductivity and higher rate of de-doping than the sample w/o AE. The UV-Vis-NIR spectrum in Fig. 1b shows slightly higher P1 absorbance and a reduction in P3 compared to the  $FeCl_3$  doped sample. This could perhaps be a sign of bipolaron formation, which could reduce the initial conductivity. This data is, however, not

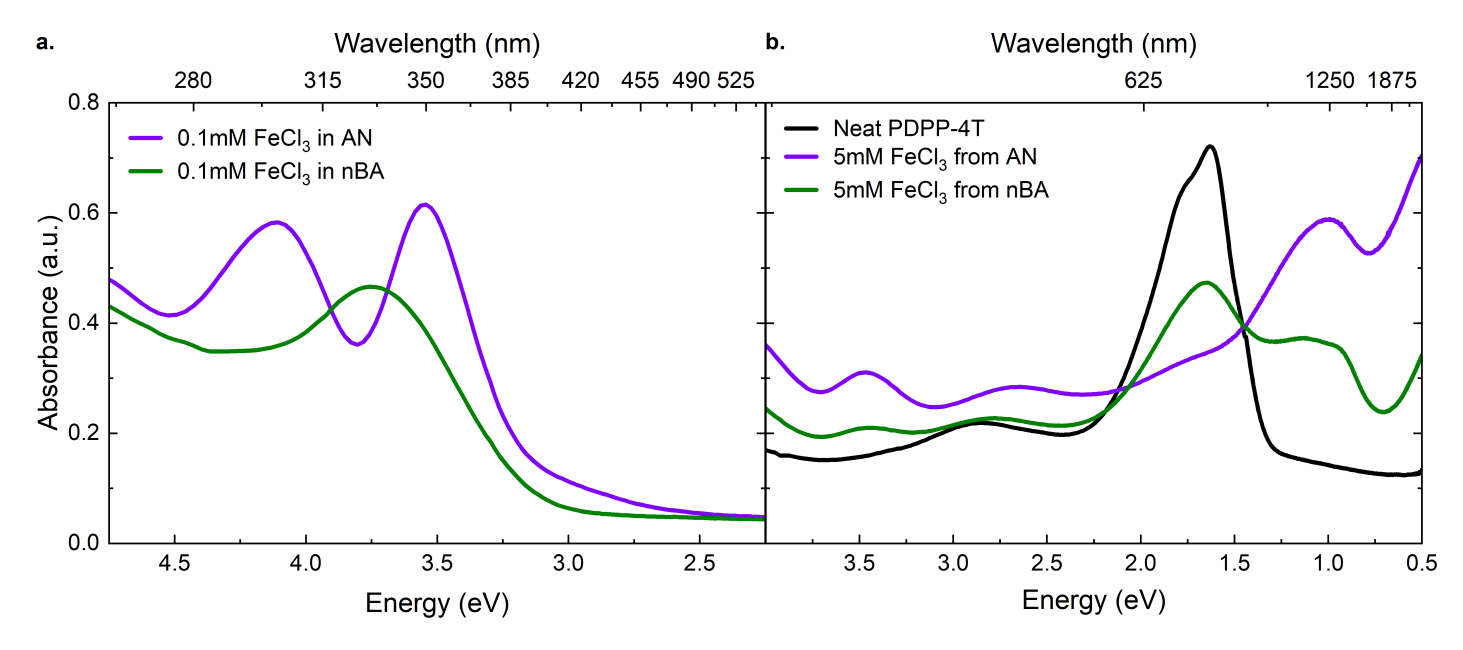


Fig. 3 a) Absorption spectrum of 0.1 mM FeCl<sub>3</sub> in acetonitrile (AN) and n-butyl acetate (nBA). b) UV-Vis-NIR absorption spectra of neat PDPP-4T (black), doped by 5 mM FeCl<sub>3</sub> from AN and nBA.

sufficient to make a meaningful assignment about bipolaron formation.<sup>34</sup> Alternatively, the lower initial conductivity could be due to increased paracrystalline disorder in the AE sample due to the larger TFSI- anion. A third possibility is that incomplete anion exchange left a mixture of [FeCl<sub>4</sub>] - and TFSI- anions in the film and the mixed anions increase the energetic entropy for holes in the polymer. 10,35-37 Since we know that AE reduces the [FeCl<sub>4</sub>] - concentration, but the degradation reaction occurs anyway, it is important to think through the possible reaction mechanisms and effect of the TFSI-. One possible explanation is that [FeCl<sub>4</sub>] - could generate chlorine radicals (Cl<sup>-</sup>) which could result in bond breaking reactions. To explore this possibility, we performed gas chromatography-mass spectrometry (GC-MS) on a mixture of anthracene, FeCl<sub>3</sub> and nBA in the presence of H<sub>2</sub>O. We chose anthracene for this experiment because it is a conjugated molecule with low molecular mass that it can be processed in GC-MS. We detected chlorinated anthracene (for details see Supporting Information Section S6) which proves the FeCl3 attacks conjugated carbon bonds and can change the nature of the polymer, which is why we see a decrease in the absorbance of the neutral peak in Fig. 1b, d. TFSI<sup>-</sup> is hydrophilic so it is possible that the degradation reaction rate is increased in the presence of TFSI- because it has a role in increasing the water uptake into the AE doped film.

#### 3.2 P3HT doped with FeCl<sub>3</sub> and F4TCNQ

It is clear from Section 3.1 that both sequential solution doping and AE doping using FeCl<sub>3</sub> as the dopant results in some side reactions that result in bond breaking reactions along the conjugated core of the polymer backbone. Our attempts to avoid this reaction by replacing the [FeCl<sub>4</sub>] $^-$  counter ion with TFSI $^-$  increased rather than decreased the rate of the degradation reaction. In this section we are switching to investigation of the polymer P3HT

(for structure refer to Fig. 1a) because it is easier to ionize and will enable doping and AE doping using F4TCNQ (for structure refer to Fig. 1a) as the reactive molecule for a comparative study against FeCl<sub>3</sub>.

Fig. 4a shows UV-Vis-NIR spectra of a P3HT film before (black spectrum) and after (solid red spectrum) sequentially doping with 0.5 mM FeCl<sub>3</sub>. Neat P3HT shows strong vibronic absorption peaks at  $\sim$ 2 (0-0),  $\sim$ 2.2 (0-1) and  $\sim$ 2.4 (0-2) eV which is in accordance with literature.<sup>38</sup> When doped with 0.5 mM FeCl<sub>3</sub>, we observe reduction of these neutral peaks and emergence of polaron peaks assigned to P3HT<sup>+</sup> at 0.42 (P1), 1.4 (P2), 1.63 (P3) eV.<sup>27</sup> In addition, the [FeCl<sub>4</sub>] - peak emerges at 3.44 eV. Fig. 4a also shows the UV-Vis-NIR spectra of P3HT doped with a mixture of 0.5 mM FeCl<sub>3</sub> + 100 mM LiTFSI (w/ AE, solid blue spectrum). Interestingly, the [FeCl<sub>4</sub>] – peak does not exist in this sample (for detailed fits see Supporting Information Fig. S4) which could point to an almost complete exchange of the [FeCl<sub>4</sub>] and TFSI ion. To test whether the low [FeCl<sub>4</sub>] - content affects the film stability, doped P3HT-FeCl<sub>3</sub> films w/o AE and w/ AE were allowed to de-dope in air while being covered to prevent exposure to light. The degradation of the doped films was monitored by periodically taking UV-Vis-NIR spectra (Fig. 4b), and four-bar conductivity measurements (Fig. 4c). Fig 4a also shows the UV-Vis-NIR spectra of the same polymer films after they were allowed to de-dope in air in the dark after almost 1000 hrs (dashed red and blue spectra). It is evident that after almost 1000 hrs, doped P3HT w/ AE has a higher polaron peak than doped P3HT w/o AE. So for the case of P3HT, AE resulted in lower [FeCl<sub>4</sub>] - concentration and reduced degradation due to the side reaction. The neutral peak in both cases reduces significantly in intensity as compared to the un-doped, neat P3HT (black spectrum), showing that the degradation reaction cannot be avoided even with very high AE ratios.

Fig. 4b is a plot of normalised O.D. of the P3HT-FeCl<sub>3</sub> polaron

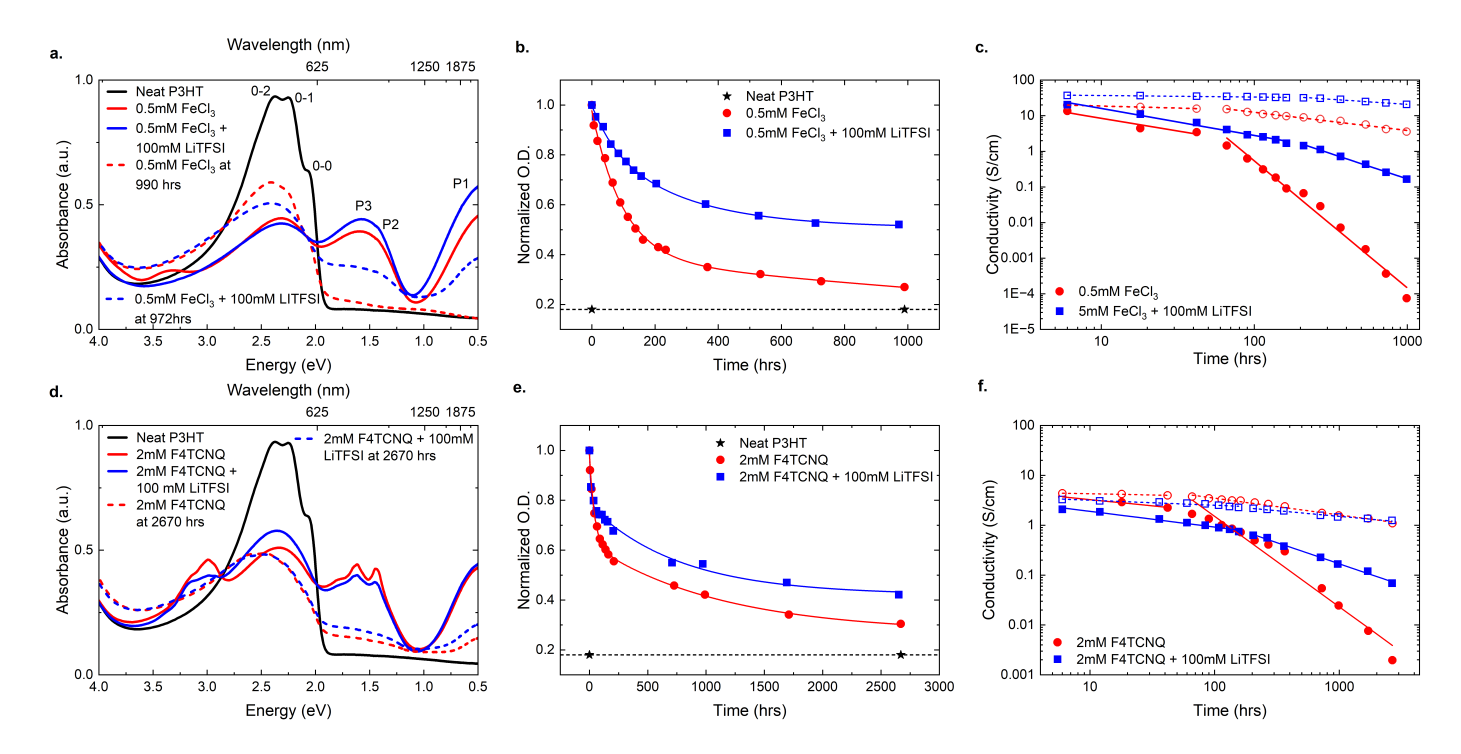


Fig. 4 a(d)) UV-Vis-NIR absorption spectra of P3HT neat (black), doped with 0.5 mM FeCl<sub>3</sub> (2 mM F4TCNQ) and either 0 (red) or 100 (blue) mM LiTFSI at t=0 (solid) and de-doped in air (dashed). b, e) Plot of normalized optical density (0.D.) of decay of the polaron peak, P3 of P3HT v/s de-doping time for a film in air. c(f)) Four probe conductivity measurements of P3HT doped with 0.5 mM FeCl<sub>3</sub> (2 mM F4TCNQ) and 0 (red) and 100 mM (blue) LiTFSI over de-doping time (Solid symbols for air and hollow symbols for  $N_2$ ).

Sample	$r_1 \left[\frac{1}{hr}\right]$	$r_2\left[\frac{1}{hr}\right]$
P3HT w/o AE in N <sub>2</sub>	0.006	0.03
P3HT w/ AE in N <sub>2</sub>	0.001	0.008
P3HT w/o AE in air	0.05	0.26
P3HT w/ AE in air	0.04	0.07

Table 2 Decay rates for degradation of P3HT doped using  $\text{FeCl}_3$  as the reactive dopant.

peak P3 at  $\sim\!1.63$  eV vs time. It shows the reduction of the polaron peak for P3HT-FeCl $_3$  w/o and w/ AE during de-doping time. The O.D. is normalized w.r.t. the polaron peak at t=0. The black stars at normalized O.D.= 0.18 represent the polaron peak of neutral P3HT. It is evident that in the span of 1000 hrs, P3HT-FeCl $_3$  w/ AE has  $\sim\!45\%$  greater polaron peak than P3HT w/o AE. The decay of the polaron peak can be fitted by an exponential function with two time constants. The details of the fits can be found in the Supporting Information Section S5.

Fig. 4c is a plot of conductivity vs time for P3HT-FeCl<sub>3</sub> w/ and w/o AE. At the same concentration of FeCl<sub>3</sub>, the P3HT-FeCl<sub>3</sub> film w/ AE (37 S/cm) has a higher initial conductivity than the film w/o AE (20 S/cm). Just like in the case of PDPP-4T there are two decay rates at shorter and longer times. The rates ( $r_1$  and  $r_2$ ) for P3HT-doped with FeCl<sub>3</sub> are in Table 2. The rate of decay for P3HT-FeCl<sub>3</sub> w/ AE is lower than that of P3HT-FeCl<sub>3</sub> w/o AE. Based on the results in Fig. 4b, c, it can be concluded that the advantages of anion exchange using FeCl<sub>3</sub> as the reactive dopant can only be realized when there is almost no [FeCl<sub>4</sub>] – left in the

polymer film.

A meaningful question that can be asked at this stage is if partial anion exchange would be detrimental to the polymer's initial conductivity and long time performance for all the dopants. Is  $FeCl_3$  the only dopant that causes side reactions and degrades the polymer faster compared to other dopants. In order to answer those questions, we doped P3HT with F4TCNQ w/ and w/o AE.

Fig. 4d is the UV-Vis-NIR spectra of P3HT, neat (black spectrum), sequentially doped with 2 mM F4TCNQ (solid red spectrum, w/o AE) and a mixture of 2 mM F4TCNO + 100 mM LiTFSI (solid blue spectrum, w/ AE). In addition to the bleaching of the neutral peaks (0-0, 0-1, 0-2) and emergence of the polaron peaks (P1, P2, P3), we also see the F4TCNQ<sup>--</sup> peaks at 1.42 and 1.6 eV in both of the doped samples, which indicates that AE is only partial for F4TCNQ<sup>--</sup> with TFSI<sup>-</sup>. Fig. 4d also shows the UV-Vis-NIR spectra after these films were allowed to de-dope in air in the dark after almost 3000 hrs (dashed red and blue spectra). Even after  $\sim$ 3000 hrs, the films were still not completely de-doped. Even with partial anion exchange, P3HT-F4TCNQ w/ AE maintains a higher doping level than P3HT-F4TCNQ w/o AE. Our comparison between PDPP-4T and P3HT shows conclusively that AE can result in higher initial conductivity and longer lifetime, but the benefit is very system dependent and also depends strongly on the processing conditions under which AE occurred. Future work on AE doping should always include multiple polymers and a simple lifetime test to determine the permanence of the doping.

Fig. 4e is a plot of normalized O.D. of the decay of the P3HT-F4TCNQ polaron peak P3 at  $\sim$ 1.63 eV vs time. The decay can be fitted by an exponential function with two time constants. It

is clear that even with incomplete anion exchange of F4TCNQ'-, P3HT-F4TCNQ w/ AE performs better than P3HT-F4TCNQ w/o AE, which did not happen in case of incomplete anion exchange of the [FeCl<sub>4</sub>]<sup>-</sup> anion. The anion exchange efficiency defines what ion ratio and how much unreacted material remains in the polymer after doping. A more complete anion exchange will minimize the amount of [FeCl<sub>4</sub>]<sup>-</sup> left in the polymer film but degradation reaction will occur even with very small quantities of [FeCl<sub>4</sub>]<sup>-</sup> (not detectable in UV-Vis-NIR spectra as in the case of P3HT-FeCl<sub>3</sub> w/ AE). This is because TFSI<sup>-</sup> ions will attract water which may lead to formations of Cl<sup>-</sup> that then react with the polymer. This data clearly shows that storing doped polymer in the glovebox results in a longer lifetime.

Fig. 4f is a plot of conductivity vs time for P3HT-F4TCNQ w/ and w/o AE. Even though the initial conductivity (at t=0) for P3HT-F4TCNQ w/o AE (4.5 S/cm) is higher than P3HT-F4TCNQ w/ AE (3.3 S/cm), conductivity after  $\sim\!\!3000$  hrs for P3HT-F4TCNQ w/o AE is two orders of magnitude higher than P3HT-F4TCNQ w/o AE.  $r_1$  and  $r_2$  values for this polymer-dopant system can be found in Table 3.

The initial decay of conductivity is considerably higher for P3HT doped with F4TCNQ vs P3HT doped with FeCl<sub>3</sub>. Recall that F4TCNQ is also not a perfect dopant. After the doping reaction, an equilibrium exits between F4TCNQ and F4TCNQ.-. F4TCNQ has a relatively high diffusion rate in P3HT driven by the fractional minority of F4TCNQ molecules that are neutral rather than charged. 16 Neutral F4TCNQ is fairly volatile (sublimes from the film) and forms charge transfer complexes with noble metals and ITO. These processes mean that the concentration of F4TCNQ<sup>--</sup> in a doped film is often reduced, thereby reducing the number of doped sites, which leads to the de-doping of the polymer film. This data shows that F4TCNQ<sup>--</sup> concentration is reduced more quickly initially than [FeCl<sub>4</sub>]-. Our assumption is that both counter ions react with H2O but F4TCNQ also sublimes out while FeCl<sub>3</sub> is non-volatile. However, removal of F4TCNQ<sup>--</sup> from the film does not result in radical side reactions, while removal of [FeCl<sub>4</sub>] - does result in the formation of radicals. This is because FeCl<sub>3</sub> undergoes a complex chemical reaction in a solvent wherein the chemical identity of the molecule is changed even before the doping reaction can happen. 8 Once the doping is done, the polymer film contains a number of iron species which could lead to the formation of Cl. which is highly reactive toward carbon-carbon double bonds. This was demonstrated by a model reaction using GC-MS (see Supporting Information Section S6). The F4TCNQ AE doped P3HT has a longer lifetime because the combination of F4TCNQ<sup>--</sup> and TFSI<sup>-</sup> ions remain stable with no side reactions while the FeCl<sub>3</sub> AE doped P3HT is slowly degraded by the radical side reaction that happens because of the instability of [FeCl<sub>4</sub>]<sup>-</sup>-TFSI<sup>-</sup>.

#### 4 Conclusions

In this article, we evaluated the stability of PDPP-4T and P3HT films doped with FeCl<sub>3</sub>. We found that degradation of conductivity, reduction in polaron absorbance, and reduced absorbance from the neutral sites of the polymer all occurred with greatly increased rates in the presence of air. The reduction of polymer

Sample	$r_1 \left[\frac{1}{hr}\right]$	$r_2\left[\frac{1}{hr}\right]$
P3HT w/o AE in N <sub>2</sub>	0.01	0.08
P3HT w/ AE in N <sub>2</sub>	0.03	0.07
P3HT w/o AE in air	0.07	0.5
P3HT w/ AE in air	0.15	0.4

Table 3 Decay rates for degradation of P3HT doped using F4TCNQ as the reactive dopant.

absorbance is attributed to formation of radicals in side reactions because of by-products of the FeCl<sub>3</sub> doping process. One route to avoid this side reaction is to use anion exchange to replace the [FeCl<sub>4</sub>] with a different counter ion before the degradation reaction can occur. The results show that an incomplete anion exchange between TFSI- and [FeCl<sub>4</sub>]- leads to significant reduction in the lifetime and conductivity of the polymer film. TFSI<sup>-</sup> is hydrophilic so it is possible that polymer degradation occurs even with fewer [FeCl<sub>4</sub>] ions because of the increase in water uptake into the film. To demonstrate that [FeCl<sub>4</sub>] is the origin of the side reaction, we compared the lifetime of P3HT doped and anion exchange doped with FeCl<sub>3</sub> and F4TCNQ. Although FeCl<sub>3</sub> resulted in an initially higher conductivity, the samples doped with F4TCNQ had more stable doping, and no evidence of polymer degradation. These results highlight that much more research is needed into stable molecular doping for long lasting organic electronic devices. FeCl<sub>3</sub> achieves high initial conductivity but results in a long term polymer degradation. F4TCNQ has insufficient electron affinity and is volatile, leading to dopant diffusion and reduced conductivity over time. Anion exchange promises better long term stability but the exchange process is never 100% complete and TFSI-, while itself being stable, may increase the hydrophilicity of the polymer film. Future studies of molecular dopants in organic materials should always include lifetime tests that enable a fuller evaluation of the usefulness of a new molecular dopant.

### Conflicts of interest

In accordance with our policy on Conflicts of interest please ensure that a conflicts of interest statement is included in your manuscript here. Please note that this statement is required for all submitted manuscripts. If no conflicts exist, please state that "There are no conflicts to declare".

#### Supporting Information

Changes in polymer film thickness upon doping, dedoping with butylamine, fitting details for PDPP-4T-FeCl $_3$  and P3HT-FeCl $_3$  series, calculation of  $r_1$  and  $r_2$ , normalized O.D. fits, GC-MS data.

#### Acknowledgements

This research was funded in main part by NSF Advanced Manufacturing award #2208009 including salary for M.J., J.M.S., and A.J.M. This research used resources of the Advanced Light Source, which is a DOE Office of Science User Facility under contract no. DE-AC02-05CH11231. L. R. F. acknowledges DOE BES DE-SC0020320.

#### Notes and references

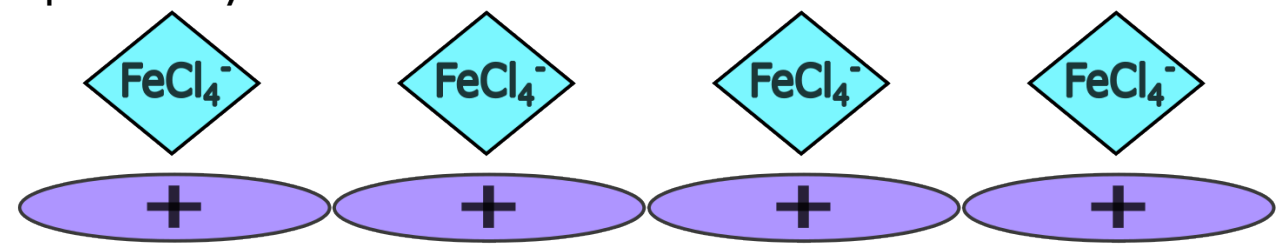
- 1 Walzer, K.; Maennig, B.; Pfeiffer, M.; Leo, K. Highly Efficient Organic Devices Based on Electrically Doped Transport Layers. *Chemical Reviews* **2007**, *107*, 1233–1271.
- 2 Lussem, B.; Keum, C.-M.; Kasemann, D.; Naab, B.; Bao, Z.; Leo, K. Doped organic transistors. *Chemical reviews* **2016**, *116*, 13714–13751.
- 3 Jacobs, I. E.; Moulé, A. J. Controlling Molecular Doping in Organic Semiconductors. *Advanced Materials* **2017**, *29*, 1703063.
- 4 Moulé, A. J.; Gonel, G.; Murrey, T. L.; Ghosh, R.; Saska, J.; Shevchenko, N. E.; Denti, I.; Fergerson, A. S.; Talbot, R. M.; Yacoub, N. L.; Mascal, M.; Salleo, A.; Spano, F. C. Quantifying Polaron Mole Fractions and Interpreting Spectral Changes in Molecularly Doped Conjugated Polymers. *Advanced Electronic Materials* **2022**, *8*, 2100888.
- 5 Fratini, S.; Nikolka, M.; Salleo, A.; Schweicher, G.; Sirringhaus, H. Charge transport in high-mobility conjugated polymers and molecular semiconductors. *NATURE MATERIALS* **2020**, *19*, 491–502.
- 6 Yamashita, Y.; Tsurumi, J.; Ohno, M.; Fujimoto, R.; Kumagai, S.; Kurosawa, T.; Okamoto, T.; Takeya, J.; Watanabe, S. Efficient molecular doping of polymeric semiconductors driven by anion exchange. *Nature* **2019**, *572*, 634–638.
- 7 Liang, Z.; Zhang, Y.; Souri, M.; Luo, X.; Boehm, A.; Li, R.; Zhang, Y.; Wang, T.; Kim, D.-Y.; Mei, J.; Marder, S. R.; Graham, K. R. Influence of dopant size and electron affinity on the electrical conductivity and thermoelectric properties of a series of conjugated polymers. *J. Mater. Chem. A* 2018, 6, 16495–16505.
- 8 Jacobs, I. E.; Lin, Y.; Huang, Y.; Ren, X.; Simatos, D.; Chen, C.; Tjhe, D.; Statz, M.; Lai, L.; Finn, P. A.; et al. High-Efficiency Ion-Exchange Doping of Conducting Polymers. *Advanced Materials* **2022**, *34*, 2102988.
- 9 Zeng, H.; Mohammed, M.; Untilova, V.; Boyron, O.; Berton, N.; Limelette, P.; Schmaltz, B.; Brinkmann, M. Fabrication of Oriented n-Type Thermoelectric Polymers by Polarity Switching in a DPP-Based Donor–Acceptor Copolymer Doped with FeCl3. *Advanced Electronic Materials* **2021**, *7*, 2000880.
- 10 Murrey, T. L.; Riley, M. A.; Gonel, G.; Antonio, D. D.; Filardi, L.; Shevchenko, N.; Mascal, M.; Moulé, A. J. Anion Exchange Doping: Tuning Equilibrium to Increase Doping Efficiency in Semiconducting Polymers. *The Journal of Physical Chemistry Letters* 2021, 12, 1284–1289, PMID: 33497232.
- 11 Aubry, T. J.; Winchell, K.; Salamat, C. Z.; Basile, V. M.; Lindemuth, J. R.; Stauber, J. M.; Axtell, J. C.; Kubena, R. M.; Phan, M. D.; Bird, M. J.; et al. Tunable dopants with intrinsic counterion separation reveal the effects of electron affinity on dopant intercalation and free carrier production in sequentially doped conjugated polymer films. *Advanced functional materials* 2020, 30, 2001800.
- 12 Thomas, E. M.; Peterson, K. A.; Balzer, A. H.; Rawlings, D.; Stingelin, N.; Segalman, R. A.; Chabinyc, M. L. Effects of Counter-Ion Size on Delocalization of Carriers and Stability

- of Doped Semiconducting Polymers. *Advanced Electronic Materials* **2020**, *6*, 2000595.
- 13 Chen, C.; Jacobs, I. E.; Kang, K.; Lin, Y.; Jellett, C.; Kang, B.; Lee, S. B.; Huang, Y.; BaloochQarai, M.; Ghosh, R.; et al. Observation of Weak Counterion Size Dependence of Thermoelectric Transport in Ion Exchange Doped Conducting Polymers Across a Wide Range of Conductivities. Advanced Energy Materials 2023, 13, 2202797.
- 14 Müller, L.; Rhim, S.-Y.; Sivanesan, V.; Wang, D.; Hietzschold, S.; Reiser, P.; Mankel, E.; Beck, S.; Barlow, S.; Marder, S. R.; Pucci, A.; Kowalsky, W.; Lovrincic, R. Electric-Field-Controlled Dopant Distribution in Organic Semiconductors. *Advanced Materials* 2017, 29, 1701466.
- 15 Li, J.; Rochester, C. W.; Jacobs, I. E.; Friedrich, S.; Stroeve, P.; Riede, M.; Moule, A. J. Measurement of Small Molecular Dopant F4TCNQ and C60F36 Diffusion in Organic Bilayer Architectures. ACS applied materials & interfaces 2015, 7, 28420–8.
- 16 Li, J.; Koshnick, C.; Diallo, S. O.; Ackling, S.; Huang, D.; Jacobs, I. E.; Harrelson, T.; Hong, K.; Zhang, G.; Beckett, J.; Mascal, M.; Moule, A. J. Quantitative Measurements of the temperature-dependent microscopic and macroscopic dynamics of a molecular dopant in a conjugated polymer. *Macromolecules* 2017, 50, 5476–5489.
- 17 Murrey, T. L.; Aubry, T. J.; Ruiz, O. L.; Thurman, K. A.; Eckstein, K. H.; Doud, E. A.; Stauber, J. M.; Spokoyny, A. M.; Schwartz, B. J.; Hertel, T.; Blackburn, J. L.; Ferguson, A. J. Tuning counterion chemistry to reduce carrier localization in doped semiconducting carbon nanotube networks. *Cell Reports Physical Science* 2023, 4, 101407.
- 18 Kratochvil, B.; Long, R. Iron(III)-(II) couple in acetonitrile. Oxidation of thiocyanate by iron(III). *Analytical Chemistry* **1970**, *42*, 43–46.
- 19 Magini, M.; Radnai, T. X-ray diffraction study of ferric chloride solutions and hydrated melt. Analysis of the iron (III)–chloride complexes formation. *The Journal of Chemical Physics* **2008**, *71*, 4255–4262.
- 20 Husain, H.; Hariyanto, B.; Sulthonul, M.; Thamatkeng, P.; Pratapa, S. Local structure examination of mineral-derived Fe2O3 powder by Fe K-edge EXAFS and XANES. IOP Conference Series: Materials Science and Engineering. 2018; p 012027.
- 21 Ray, S.; Tsai, H.; Pao, C.; Chang, W.; Pong, W.; Chiou, J.; Tsai, M.-H. Electronic and bonding properties of Fe-and Ni based hydrogenated amorphous carbon thin films by X-ray absorption, valence-band photoemission and Raman spectroscopy. *Diamond and related materials* **2011**, *20*, 886–890.
- 22 Heintges, G. H.; Leenaers, P. J.; Janssen, R. A. The effect of side-chain substitution and hot processing on diketopyrrolopyrrole-based polymers for organic solar cells. *Journal of Materials Chemistry A* **2017**, *5*, 13748–13756.
- 23 Hofmann, A. I.; Kroon, R.; Zokaei, S.; Järsvall, E.; Malacrida, C.; Ludwigs, S.; Biskup, T.; Müller, C. Chemical doping of conjugated polymers with the strong oxidant magic blue. *Advanced Electronic Materials* **2020**, *6*, 2000249.

- 24 Hestand, N. J.; Spano, F. C. Expanded theory of H-and Jmolecular aggregates: the effects of vibronic coupling and intermolecular charge transfer. Chemical reviews 2018, 118, 7069-7163.
- 25 Chang, X.; Balooch Qarai, M.; Spano, F. C. HJ-aggregates of donor-acceptor-donor oligomers and polymers. The Journal of Chemical Physics 2021, 155, 034905.
- 26 Balooch Qarai, M.; Chang, X.; Spano, F. Vibronic exciton model for low bandgap donor-acceptor polymers. The Journal of Chemical Physics 2020, 153, 244901.
- 27 Spano, F. C. The spectral signatures of Frenkel polarons in H-and J-aggregates. Accounts of chemical research 2010, 43, 429-439.
- 28 Pingel, P.; Schwarzl, R.; Neher, D. Effect of molecular p-doping on hole density and mobility in poly(3hexylthiophene). Applied Physics Letters 2012, 100, 143303.
- 29 Salzmann, I.; Heimel, G.; Oehzelt, M.; Winkler, S.; Koch, N. Molecular Electrical Doping of Organic Semiconductors: Fundamental Mechanisms and Emerging Dopant Design Rules. Accounts of Chemical Research 2016, 49, 370–378.
- 30 Swanson, T. B.; Laurie, V. W. Electron Magnetic Resonance and Electronic Spectra of Tetrachloroferrate(III) Ion in Nonaqueous Solution1. The Journal of Physical Chemistry 1965, 69, 244-250.
- 31 Jacobs, I. E.; Wang, F.; Hafezi, N.; Medina-Plaza, C.; Harrelson, T. F.; Li, J.; Augustine, M. P.; Mascal, M.; Moulé, A. J. Quantitative dedoping of conductive polymers. Chemistry of Materials 2017, 29, 832-841.
- 32 Saravanan, K.; Jayalakshmi, G.; Suresh, K.; Sundaravel, B.; Panigrahi, B.; Phase, D. Structural evaluation of reduced

- graphene oxide in graphene oxide during ion irradiation: Xray absorption spectroscopy and in-situ sheet resistance studies. Applied Physics Letters 2018, 112, 111907.
- 33 Wang, D.; Yang, J.; Li, X.; Geng, D.; Li, R.; Cai, M.; Sham, T.-K.; Sun, X. Layer by layer assembly of sandwiched graphene/SnO 2 nanorod/carbon nanostructures with ultrahigh lithium ion storage properties. Energy & Environmental Science 2013, 6, 2900-2906.
- 34 Voss, M. G.; Challa, J. R.; Scholes, D. T.; Yee, P. Y.; Wu, E. C.; Liu, X.; Park, S. J.; León Ruiz, O.; Subramaniyan, S.; Chen, M.; Jenekhe, S. A.; Wang, X.; Tolbert, S. H.; Schwartz, B. J. Driving Force and Optical Signatures of Bipolaron Formation in Chemically Doped Conjugated Polymers. Advanced Materials **2021**, 33, 2000228.
- 35 Paulsen, B. D.; Frisbie, C. D. Dependence of conductivity on charge density and electrochemical potential in polymer semiconductors gated with ionic liquids. The Journal of Physical Chemistry C 2012, 116, 3132-3141.
- 36 Arkhipov, V.; Emelianova, E.; Heremans, P.; Bässler, H. Analytic model of carrier mobility in doped disordered organic semiconductors. Physical Review B 2005, 72, 235202.
- 37 Jacobs, I. E.; D'avino, G.; Lemaur, V.; Lin, Y.; Huang, Y.; Chen, C.; Harrelson, T. F.; Wood, W.; Spalek, L. J.; Mustafa, T.; et al. Structural and dynamic disorder, not ionic trapping, controls charge transport in highly doped conducting polymers. Journal of the American Chemical Society 2022, 144, 3005-3019.
- 38 Niles, E. T.; Roehling, J. D.; Yamagata, H.; Wise, A. J.; Spano, F. C.; Moule, A. J.; Grey, J. K. J-aggregate behavior in poly-3-hexylthiophene nanofibers. Journal of Physical Chemistry Letters 2012, 3, 259-263.

# Doped Polymer



Doped Polymer +  $H_2O/O_2$  + Time  $\longrightarrow$  De-doped Polymer

# De-doped Polymer

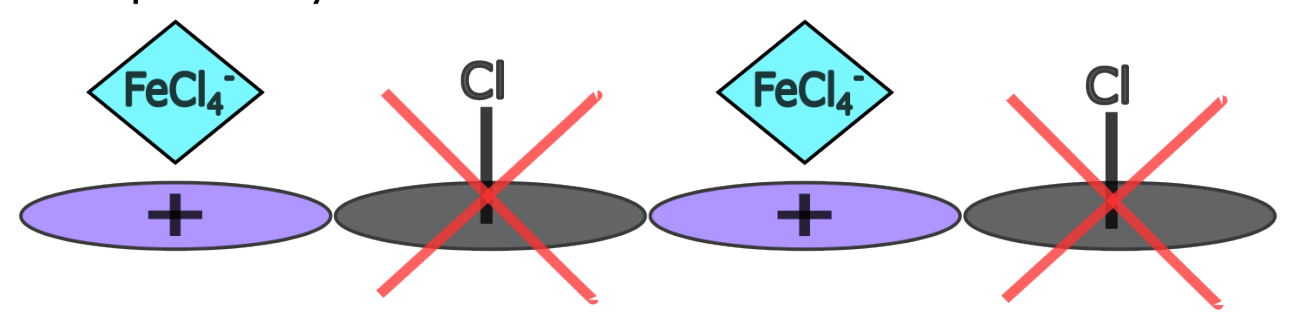


Fig. 5 TOC Graphic